Frontiers of Information Technology & Electronic Engineering
www.jzus.zju.edu.cn; engineering.cae.cn; www.springerlink.com
ISSN 2095-9184 (print); ISSN 2095-9230 (online)
E-mail: jzus@zju.edu.cn

Generalized labeled multi-Bernoulli filter with signal features of unknown emitters*

Qiang GUO†1, Long TENG†‡1,2, Xinliang WU†2, Wenming SONG†2, Dayu HUANG2

[1]*College of Information and Communication Engineering, Harbin Engineering University, Harbin 150001, China*

[2]*China National Aeronautical Radio Electronics Research Institute, Shanghai 200233, China*

†E-mail: guoqiang@hrbeu.edu.cn; tenglong@hrbeu.edu.cn; wuxinliang51@163.com; hdayady@163.com

Received June 30, 2022; Revision accepted Oct. 10, 2022; Crosschecked Oct. 27, 2022

Abstract: A novel algorithm that combines the generalized labeled multi-Bernoulli (GLMB) filter with signal features of the unknown emitter is proposed in this paper. In complex electromagnetic environments, emitter features (EFs) are often unknown and time-varying. Aiming at the unknown feature problem, we propose a method for identifying EFs based on dynamic clustering of data fields. Because EFs are time-varying and the probability distribution is unknown, an improved fuzzy C-means algorithm is proposed to calculate the correlation coefficients between the target and measurements, to approximate the EF likelihood function. On this basis, the EF likelihood function is integrated into the recursive GLMB filter process to obtain the new prediction and update equations. Simulation results show that the proposed method can improve the tracking performance of multiple targets, especially in heavy clutter environments.

Key words: Multi-target tracking; Generalized labeled multi-Bernoulli; Signal features of emitter; Fuzzy C-means; Dynamic clustering

https://doi.org/10.1631/FITEE.2200286 **CLC number:** TN953

1 Introduction

The objective of multi-target tracking is to transform uncertain measurement information into deterministic target state information. At present, multi-target tracking methods include two categories: (1) data association algorithms (Guo YF et al., 2015), such as probabilistic data association (PDA) (Guo YF et al., 2016), joint PDA (JPDA) (Guo YF et al., 2020a, 2020b; Zhu Y et al., 2021), and multiple hypotheses tracking (MHT) (Chen et al., 2004, 2008); (2) random finite set (RFS) methods (Mahler RPS, 2007; Da et al., 2021). The former requires complex data association operations. The latter models the state and measurement information of the target as an RFS, which can effectively avoid the complex data correlation process and is a popular multi-target tracking method nowadays. The core of the RFS is the Bayesian multi-objective filter, which propagates the posterior density of multi-objective states recursively in time.

Because Bayesian multi-objective filters do not have closed solutions, approximation methods such as probability hypothesis density (PHD), cardinality PHD (CPHD), and multi-Bernoulli (MB) filters have been proposed one after another (Mahler RPS, 2003; Mahler R, 2007; Ristic et al., 2013). It is assumed that the multi-object probability distribution in PHD and CPHD filters is a Poisson process and an independent and identically distributed process, respectively. PHD and CPHD filters recursively

‡ Corresponding author

* Project supported by the National Major Research and Development Project of China (No. 2018YFE0206500), the National Natural Science Foundation of China (No. 62071140), the International Scientific and Technological Cooperation Program of China (No. 2015DFR10220), and the Technology Foundation for Basic Enhancement Plan, China (No. 2021-JCJQ-JJ-0301)

ORCID: Qiang GUO, https://orcid.org/0000-0002-8366-7163; Long TENG, https://orcid.org/0000-0003-3519-7790

propagate the combination of the statistical moments and cardinality distribution of the posterior distribution. It is assumed that the multi-target probability distribution in the MB filter is an MB process, and the MB filter directly approximates the multi-objective probability distribution and recurses the parameters of the MB distribution. Implementations of these filters include Gaussian mixture (GM) and sequential Monte Carlo (SMC) (Vo and Ma, 2006; Li et al., 2016), as well as multiple extended versions (Li et al., 2017, 2018; Wang et al., 2021), such as distributed PHD/CPHD filter (Battistelli et al., 2013; Da et al., 2020; Yi et al., 2020; Li and Hlawatsch, 2021; Yi and Chai, 2021) and distributed Bernoulli filter (Li et al., 2019). However, these filters cannot directly form track information.

To address the inherent drawback of the above filters, Vo et al. (2014) introduced a conjugate prior based on the Chapman–Kolmogorov equation to derive a multi-target tracking algorithm for obtaining target track labels, i.e., the generalized labeled multi-Bernoulli (GLMB) filter. Vo et al. (2017) further improved the real-time performance of the GLMB filter by combining the prediction and update steps and introducing Gibbs sampling to truncate the density. More extended applications have been developed, such as the multi-model GLMB filter (Yi et al., 2017; Wu et al., 2021) and the distributed GLMB filter (Herrmann et al., 2021).

However, as the number of clutters in the target tracking scene increases, the differentiation between the target measurement and the clutter gradually decreases. The tracking performance of the above RFS filters will be degraded to different degrees. To improve the anti-clutter performance of RFS filters, some algorithms integrate multi-dimensional independent information into the RFS filters. Bar-Shalom et al. (2005) proposed a target tracking algorithm with classification information by integrating target classification information into the data association process. In the target tracking scenarios, the amplitude of the target echo is stronger than those coming from clutter. Clark et al. (2010) proved that the amplitude information of the target echo can improve the multi-target state estimation accuracy, and applied it to PHD and CPHD filters under Gaussian conditions. Similarly, amplitude information was integrated into MB and GLMB filters to improve multi-target tracking performance in the literature (Liu C et al., 2018; Peng et al., 2018; Sun et al., 2020). Doppler information was also widely employed in multi-target tracking (Peng et al., 2018; Jin et al., 2019).

In a multi-heterogeneous sensor tracking system, we can not only obtain the target's kinetic information (Cao and Zhao, 2022), but also intercept the emitter features (EFs) which are called the pulse description words (PDWs), such as radio frequency (RF), pulse width (PW), and pulse repetition frequency (PRF). Each feature reflects the electromagnetic characteristics of the emitter in different dimensions, and plays a vital role in the classification and identification of the emitter. RF is the frequency at which electromagnetic waves are emitted, and is closely related to the working state and modulation mode of the emitter. PW is the duration of the transmitted pulse to the maximum value. PRF determines the maximum unambiguity range and radial velocity of the radar. To our knowledge, there are few studies of RFS filters with EFs; Zhou and Zhu (2015) and Zhu YQ (2015) are the only ones in which EFs were integrated in a PHD filter with the prerequisite that the EFs are known and non-time-varying. The filter does not form track information.

In a real target tracking scenario, the target track is necessary and the EFs are usually unknown and time-varying. In this paper, the state and measurement of the target are extended, and the EF identification method based on dynamic clustering of the data field is proposed to solve the problem of unknown EF. On this basis, an improved fuzzy C-means (FCM) algorithm is proposed, which can approximately calculate the time-varying EF likelihood and solve the problems that EFs are time-varying and the probability distribution is unknown. Then the EFs are integrated into the GLMB filter to solve the problem that the track cannot be generated directly. The filter proposed in this paper can improve multi-target tracking performance, especially in heavy clutter environments.

2 Background

We briefly review the GLMB filter, including labeled RFS, multi-object state transition model, multi-object observation model, and GLMB. Readers can refer to Vo et al. (2014) for details.

2.1 Labeled RFS

Denote $\mathbb{X}$ as the single target state space and $\mathbb{L}$ as the discrete label space. $\mathcal{L}:\mathbb{X}\times\mathbb{L}\to\mathbb{L}$ is the projection defined by $\mathcal{L}((x,\ell))=\ell$. Then $\mathcal{L}(X)$ is called the label of point $\boldsymbol{x}\in\mathbb{X}\times\mathbb{L}$. A finite subset X of $\mathbb{X}\times\mathbb{L}$ is said to have distinct labels if and only if X and its labels $\mathcal{L}(X)=\{\mathcal{L}(\boldsymbol{x}):\boldsymbol{x}\in X\}$ have the same cardinality. The available label indicator function is defined as

$$\Delta(X)\triangleq\delta_{|X|}[|\mathcal{L}(X)|], \tag{1}$$

where $|X|$ is the cardinality distribution.

2.2 Multi-object state transition model

Given the multi-object state X, each $(x,\ell)\in X$ either survives with probability $P_{\mathrm{s}}(x,\ell)$ and propagates to get a new state (x_+,ℓ_+), or dies with probability $1-P_{\mathrm{s}}(x,\ell)$. For notational compactness, the subscript k for the time index is omitted and the subscript "+" is used to denote the next time. The new state includes the objects of survival and new birth. The set B_+ of the new birth objects is distributed according to the labeled multi-Bernoulli (LMB) density:

$$\begin{aligned}f_{B_+}(B_+)=&\Delta(B_+)\left[1_{\mathbb{B}_+}r_{B,+}\right]^{\mathcal{L}(B_+)}\\&\cdot\left[1-r_{B,+}\right]^{\mathbb{B}_+-\mathcal{L}(B_+)}p_{B,+}^{B_+},\end{aligned} \tag{2}$$

where $r_{B,+}(\ell)$ is the probability of the birth object with label ℓ, $p_{B,+}(\cdot,\ell)$ is the distribution of the corresponding kinetic states, and $\mathbb{B}$ is the label space for the birth objects. Assuming that the target's move, birth, and death are independent of each other, the multi-object transition density is (Vo et al., 2014)

$$\begin{aligned}f_+(X_+|X)=&f_{\mathrm{s},+}(X_+\cap\mathbb{X}\times\mathbb{L}|X)\\&\cdot f_{\mathrm{b},+}(X_+-(\mathbb{X}\times\mathbb{L})),\end{aligned} \tag{3}$$

where $f_{\mathrm{s},+}(\cdot)$ and $f_{\mathrm{b},+}(\cdot)$ represent the density functions of the surviving target and the birth target, respectively. X_+ is the multi-target state at the next time, and

$$f_{\mathrm{s},+}(W|X)=\Delta(W)\Delta(X)1_{\mathcal{L}(X)}(\mathcal{L}(W))[\Phi(W;\cdot)]^X, \tag{4}$$

$$\begin{aligned}\Phi(W;x,\ell)=&\left(1-1_{\mathcal{L}(W)}(\ell)\right)(1-P_{\mathrm{s}}(x,\ell))\\&+\sum_{(x_+,\ell_+)\in W}\delta_\ell[\ell_+]P_{\mathrm{s}}(x,\ell)f_+(x_+|x,\ell),\end{aligned} \tag{5}$$

where $1_{\mathcal{L}(X)}(\mathcal{L}(W))$ is the generalization of the indicator function. When $\mathcal{L}(X)\subseteq\mathcal{L}(W)$, $1_{\mathcal{L}(X)}(\mathcal{L}(W))=1$; otherwise, $1_{\mathcal{L}(X)}(\mathcal{L}(W))=0$. $\Delta(\cdot)$ is the distinct label indicator function. $P_{\mathrm{s}}(x,\ell)$ is the target survival probability. When $\ell_+=\ell$, we have $\delta_\ell[\ell_+]=1$. $f_+(x_+|x,\ell)$ represents the state transition function.

2.3 Multi-object observation model

Given the multi-object state X, each $(x,\ell)\in X$ is either detected with probability $P_{\mathrm{D}}(x,\ell)$ or missed with probability $1-P_{\mathrm{D}}(x,\ell)$. The multi-target observation set consists of detected objects and Poisson clutter (density $\mathcal{K}$). Assuming that the detections are independent of each other and of clutter, the multi-object likelihood function is given by (Vo et al., 2014)

$$g(Z|X)=\sum_{\theta\in\Theta(\mathcal{L}(X))}\prod_{(x,\ell)\in X}\psi_Z^{(\theta(\ell))}(x,\ell), \tag{6}$$

where Θ is the set of positive $1-1$ maps $\theta:\mathbb{L}\to\{0:|Z|\}$, and

$$\psi_Z^{(\theta(\ell))}(x,\ell)=\begin{cases}\frac{P_{\mathrm{D}}(x,\ell)g\left(z_{\theta(\ell)}|x,\ell\right)}{\mathcal{K}\left(z_{\theta(\ell)}\right)}, & \theta(\ell)>0,\\1-P_{\mathrm{D}}(x,\ell), & \theta(\ell)=0.\end{cases} \tag{7}$$

Here, map θ represents that ℓ generates detection $z_{\theta(\ell)}\in Z$ with $\theta(\ell)=0$ if ℓ is undetected, and any measurement is assigned to at most one object.

2.4 GLMB

An effective implementation of GLMB is δ-GLMB, which is a special GLMB. In this study, δ-GLMB is abbreviated as GLMB and its density is defined by

$$\pi(X)=\Delta(X)\sum_{\xi\in\Xi,I\in\mathcal{F}(\mathbb{L})}\omega^{(I,\xi)}\delta_I[\mathcal{L}(X)]\left[p^{(\xi)}\right]^X, \tag{8}$$

where $\omega^{(I,\xi)}$ and $p^{(\xi)}(\cdot,\ell)$ are the weights and probability density functions respectively, and $\sum\omega^{(I,\xi)}=1$. ξ is the history of association maps, and I is the set of object labels.

The cardinality distribution of the GLMB is given by

$$\Pr(|X|=n)=\sum_{I,\xi}\delta_n[|I|]\omega^{(I,\xi)}, \tag{9}$$

while the existence probability and probability density of the track with label ℓ are

$$r(\ell)=\sum_{I,\xi}1_I(\ell)\omega^{(I,\xi)}, \tag{10}$$

$$p(x,\ell)=\frac{1}{r(\ell)}\sum_{I,\xi}1_I(\ell)\omega^{(I,\xi)}p^{(\xi)}(x,\ell). \tag{11}$$

3 GLMB filter with EFs

This section describes the implementation of the GLMB filter with EFs. Section 3.1 gives the likelihood approximation calculations for the EFs. The recursive process of the GLMB filter with EFs is shown in Section 3.2.

3.1 Likelihood approximation of EFs

Due to the complexity of the real electromagnetic environment, EFs are usually unknown and time-varying, and their distribution is also unknown. Therefore, the likelihood of the emitters is not directly available. To address these issues, dynamic clustering based on data fields is first used to estimate the EFs. Then, inspired by PDA (it considers that all measurements can be derived from the target with different probabilities), an improved FCM algorithm is proposed to approximate the correlation weights of measurements with respect to the target and clutter, i.e., the EF likelihood.

3.1.1 EF estimation

The core idea of dynamic clustering based on data fields is to treat the EF samples as particles with mass. Dynamic clustering can radiate energy into the feature space, thus creating a data field. According to the data field principle, the samples in the feature space interact with each other. The dynamic clustering is accomplished by moving to different clustering centers under the action of field forces (Guo Q et al., 2016).

Given a set $\{\boldsymbol{v}_1,\boldsymbol{v}_2,\cdots,\boldsymbol{v}_N\}$ of EF samples, where $\boldsymbol{v}_i$ $(i=1,2,\cdots,N)$ is the position vector including the RF, PW, and PRF information, according to the nuclear radiation field model, the potential function of any position vector $\boldsymbol{v}$ is

$$\varphi(\boldsymbol{v})=\sum_{i=1}^{N}\varphi_i(\boldsymbol{v})=\sum_{i=1}^{N}m_i\mathrm{e}^{-(\|\boldsymbol{v}-\boldsymbol{v}_i\|/\sigma)^2}, \tag{12}$$

where m_i is the mass of feature i, and $\sum_{i=1}^{N}m_i=1$. "$\|\cdot\|$" represents the Euclidean distance. σ is the impact factor, controlling the range of effect on the data sample. Based on Eq. (12), the field intensity of target $\boldsymbol{v}_i$ at time t is

$$F^{(t)}(\boldsymbol{v}_i)=m_i\sum_{j=1}^{N}m_j\boldsymbol{r}_{ij}(t)\mathrm{e}^{-(\|\boldsymbol{r}_{ij}(t)\|/\sigma)^2},j\neq i, \tag{13}$$

where $\boldsymbol{r}_{ij}(t)$ is the distance vector between targets $\boldsymbol{v}_i$ and $\boldsymbol{v}_j$. Each target moves in the direction of the larger potential value under the action of the field force. After many iterations, we will obtain the cluster centers of the EFs. Fig. 1 shows an example of dynamic clustering. Each of the equipotential lines has the same potential value. The local maximum potential value surrounded by equipotential lines is called the potential center. Usually, the potential

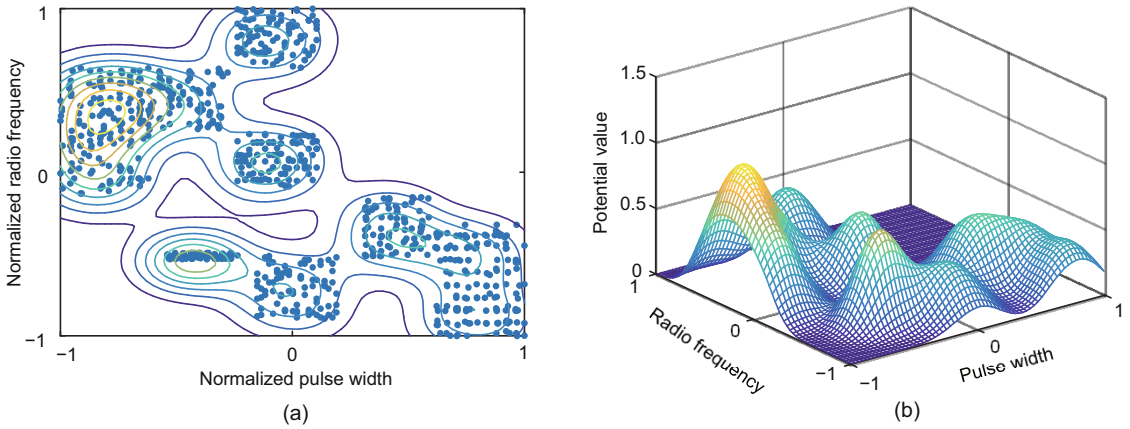

Fig. 1 An example of dynamic clustering: (a) potential field formed by the data sample in a two-dimensional space; (b) potential value of the data sample

center is located at the center of the data sample, so the potential center is often regarded as the cluster center of the data sample.

3.1.2 Likelihood calculation of the EFs

The EFs obtained in Section 3.1.1 are usually time-varying and their density distribution is unknown. Inspired by PDA (all measurements in the correlation gate can originate from the target with different probabilities; i.e., each measurement can be associated with both target and clutter), an improved FCM algorithm is proposed. It can approximate the likelihood of EFs by calculating the correlation coefficient of the measurement with respect to the target and clutter. Because the FCM algorithm is a data clustering method based on the optimization of the objective function, the clustering result is the degree of correlation of each sample to the cluster center. The concept of correlation degree is the same as the concept of likelihood in this study. They are all correlation coefficients between the measurement and the target. The objective function of the FCM clustering algorithm can be given by

$$J=\sum_{i=1}^{n_{\mathrm{s}}}\sum_{j=1}^{n_{\mathrm{c}}}\mu_{ij}^{m}d_{ij}^{2}, \tag{14}$$

where n_{s} and n_{c} represent the numbers of samples and clusters respectively, m is the weighted index, $\mu_{ij}\in[0,1]$ denotes the correlation coefficient between sample i and cluster j, and d_{ij} represents the distance between sample i and cluster j. To optimize the objective function J, the correlation coefficient is given by a Lagrange multiplier algorithm:

$$\mu_{ij}=\frac{1}{\sum_{k=1}^{n_{\mathrm{c}}}\left(\frac{d_{ij}}{d_{ik}}\right)^{2/(m-1)}}=\frac{\left(d_{ij}^{2}\right)^{1/(1-m)}}{\sum_{k=1}^{n_{\mathrm{c}}}\left(d_{ik}^{2}\right)^{1/(1-m)}}. \tag{15}$$

In the GM implementation, each Gaussian component of the predicted intensity represents a candidate target, so the feature parameter corresponding to each Gaussian component can be treated as a center of the cluster. The correlation coefficient of each measurement with respect to the target and clutter can be calculated based on the center of the cluster.

Assume that the feature measurement set at time k is $\left\{\boldsymbol{e}_{k}^{(i)}=\left(\mathrm{rf}'_{k,i},\mathrm{prf}'_{k,i},\mathrm{pw}'_{k,i}\right)\right\}_{i=1}^{N_{k}^{\mathrm{e}}}$, where N_{k}^{e} is the number of measurement points. Because the three-dimensional features of RF, PRF, and PW can be processed independently, we take RF as an example to illustrate the calculation process of the correlation coefficient, and then fuse the correlation coefficient of the three-dimensional features.

However, the time-varying features lead to the time-varying center of the cluster. We need to calculate the optimal center of the cluster at each time. First, a set of cluster center candidates is established which contains all possible values of RF features. It has been obtained in Section 3.1.1:

$$\begin{aligned}E_{\mathrm{center}}=\big\{&\left(\mathrm{rf}_{\mathrm{center}_1},\mathrm{rf}_{\mathrm{center}_2},\cdots,\mathrm{rf}_{\mathrm{center}_{l1}}\right)_1,\\&\left(\mathrm{rf}_{\mathrm{center}_1},\mathrm{rf}_{\mathrm{center}_2},\cdots,\mathrm{rf}_{\mathrm{center}_{l2}}\right)_2,\cdots,\\&\left(\mathrm{rf}_{\mathrm{center}_1},\mathrm{rf}_{\mathrm{center}_2},\cdots,\mathrm{rf}_{\mathrm{center}_{ln}}\right)_{J_k}\big\},\end{aligned} \tag{16}$$

where $\mathrm{rf}_{\mathrm{center}}$ is the cluster center of the RF features, and J_k is the number of candidate targets at time k. Then, we take a sample as an example to calculate the correlation coefficient of each cluster center in E_{center}:

$$\begin{aligned}\mu_{i,\mathrm{center}}=\big\{&\left(\mu_{i,\mathrm{center}_1},\mu_{i,\mathrm{center}_2},\cdots,\mu_{i,\mathrm{center}_{l1}}\right)_1,\\&\left(\mu_{i,\mathrm{center}_1},\mu_{i,\mathrm{center}_2},\cdots,\mu_{i,\mathrm{center}_{l2}}\right)_2,\cdots,\\&\left(\mu_{i,\mathrm{center}_1},\mu_{i,\mathrm{center}_2},\cdots,\mu_{i,\mathrm{center}_{ln}}\right)_{J_k}\big\}.\end{aligned} \tag{17}$$

According to the principle of the maximum correlation coefficient, the optimal cluster center $\mathrm{rf}_{\mathrm{center}}=\{\mathrm{rf}_{k,1},\mathrm{rf}_{k,2},\cdots,\mathrm{rf}_{k,J_k}\}$ of each candidate target is obtained. The corresponding distance matrix is given by

$$\boldsymbol{D}_{\mathrm{rf}}=\begin{pmatrix}d_{10}^{2}&d_{11}^{2}&\cdots&d_{1J_k}^{2}\\d_{20}^{2}&d_{21}^{2}&\cdots&d_{2J_k}^{2}\\\vdots&\vdots&&\vdots\\d_{N_k^{\mathrm{e}}0}^{2}&d_{N_k^{\mathrm{e}}1}^{2}&\cdots&d_{N_k^{\mathrm{e}}J_k}^{2}\end{pmatrix}, \tag{18}$$

where

$$d_{ij}^{2}=\begin{cases}\left\|\mathrm{rf}'_{k,i}-\mathrm{rf}_{k,j}\right\|^{2}, & j\neq 0,\\\left\|\Delta_{\mathrm{rf}}\right\|^{2}, & j=0.\end{cases} \tag{19}$$

Here, Δ_{rf} is the resolution about RF. Finally, the correlation coefficient matrix $\boldsymbol{U}_{\mathrm{rf}}$ of the RF feature is

$$\boldsymbol{U}_{\mathrm{rf}}=\begin{pmatrix}\mu_{10}^{\mathrm{rf}}&\mu_{11}^{\mathrm{rf}}&\cdots&\mu_{1J_k}^{\mathrm{rf}}\\\mu_{20}^{\mathrm{rf}}&\mu_{21}^{\mathrm{rf}}&\cdots&\mu_{2J_k}^{\mathrm{rf}}\\\vdots&\vdots&&\vdots\\\mu_{N_k^{\mathrm{e}}0}^{\mathrm{rf}}&\mu_{N_k^{\mathrm{e}}1}^{\mathrm{rf}}&\cdots&\mu_{N_k^{\mathrm{e}}J_k}^{\mathrm{rf}}\end{pmatrix}. \tag{20}$$

In $\boldsymbol{U}_{\mathrm{rf}}$, μ_{i0}^{rf} represents the correlation coefficient of measurement i with respect to the clutter. Similarly, we can obtain the correlation coefficient matrices of PRI and PW as $\boldsymbol{U}_{\mathrm{prf}}$ and $\boldsymbol{U}_{\mathrm{pw}}$, respectively. Therefore, for arbitrary feature measurements, the likelihoods of EFs with respect to the candidate target and clutter can be approximately calculated by fusing different features (RF, PRF, and PW):

$$g_k = \frac{\mu_{ij}^{\mathrm{rf}}\mu_{ij}^{\mathrm{prf}}\mu_{ij}^{\mathrm{pw}}}{\sum_{l=0}^{J_k}\mu_{il}^{\mathrm{rf}}\mu_{il}^{\mathrm{prf}}\mu_{il}^{\mathrm{pw}}}, \tag{21}$$

$$c_k = \frac{\mu_{i0}^{\mathrm{rf}}\mu_{i0}^{\mathrm{prf}}\mu_{i0}^{\mathrm{pw}}}{\sum_{l=0}^{J_k}\mu_{il}^{\mathrm{rf}}\mu_{il}^{\mathrm{prf}}\mu_{il}^{\mathrm{pw}}}. \tag{22}$$

3.2 Recursive process of the GLMB filter with EFs

The signal features of the radar emitter are usually highly related to the actual application of the radar, and are not necessarily related to whether the platform is moving. Therefore, we consider the EFs and the target kinetic information to be independent.

The state and measurement of the target are augmented. The augmented state $\tilde{\boldsymbol{x}}$ and measurement $\tilde{\boldsymbol{z}}$ include not only kinetic information but also EF information:

$$\tilde{\boldsymbol{x}} = [\boldsymbol{x}; \boldsymbol{x}_{\mathrm{e}}], \quad \tilde{\boldsymbol{z}} = [\boldsymbol{z}; \boldsymbol{z}_{\mathrm{e}}], \tag{23}$$

where $\boldsymbol{x}$ and $\boldsymbol{z}$ represent the target kinetic state and measurement respectively, and $\boldsymbol{x}_{\mathrm{e}}$ and $\boldsymbol{z}_{\mathrm{e}}$ indicate the EF state and measurement information respectively.

Given the GLMB filtering density (Eq. (8)) at time k, the likelihood of the EFs in Section 3.1 is integrated into the GLMB recursion (Vo et al., 2017). The GLMB filtering density at time $k+1$ is given by

$$\begin{aligned}\pi_{Z_+}(X) \propto \Delta(X) &\sum_{I,\xi,I_+,\theta_+} \omega^{(I,\xi)}\omega_{Z_+}^{(I,\xi,I_+,\theta_+)} \\ &\cdot\delta_{I_+}[\mathcal{L}(X)]\left[p_{Z_+}^{(\xi,\theta_+)}\right]^X,\end{aligned} \tag{24}$$

where $I \in \mathcal{F}(\mathbb{L}), \xi \in \Xi, I_+ \in \mathcal{F}(\mathbb{L}_+), \theta_+ \in \Theta_+$, and

$$\begin{aligned}\omega_{Z_+}^{(I,\xi,I_+,\theta_+)} =& 1_{\Theta_+(I_+)}(\theta_+)\left[1-\bar{P}_{\mathrm{s}}^{(\xi)}\right]^{I-I_+}\left[\bar{P}_{\mathrm{s}}^{(\xi)}\right]^{I\cap I_+} \\ &\cdot\left[1-r_{B,+}\right]^{\mathbb{B}_+-I_+} r_{B,+}^{\mathbb{B}_+\cap I_+}\left[\bar{\psi}_{Z_+}^{(\xi,\theta_+)}\right]^{I_+},\end{aligned} \tag{25}$$

$$\bar{P}_{\mathrm{s}}^{(\xi)}(\ell) = \left\langle p^{(\xi)}(\cdot,\ell), P_{\mathrm{s}}(\cdot,\ell)\right\rangle, \tag{26}$$

$$\bar{\psi}_{Z_+}^{(\xi,\theta_+)}(\ell_+) = \left\langle \bar{p}_+^{(\xi)}(\cdot,\ell_+), \psi_{Z_+}^{(\theta_+(\ell_+))}(\cdot,\ell_+)\right\rangle, \tag{27}$$

$$\begin{aligned}&\bar{p}_+^{(\xi)}(x_+,\ell_+) \\ =&1_{\mathbb{L}}(\ell_+)\frac{\left\langle P_{\mathrm{s}}(\cdot,\ell) f_+(x_+\mid\cdot,\ell_+), p^{(\xi)}(\cdot,\ell_+)\right\rangle}{\bar{P}_{\mathrm{s}}^{(\xi)}(\ell_+)} \\ &+1_{\mathbb{B}_+}(\ell_+)\, p_{B,+}(x_+,\ell_+),\end{aligned} \tag{28}$$

$$p_{Z_+}^{(\xi,\theta_+)}(x_+,\ell_+) = \frac{\bar{p}_+^{(\xi)}(x_+,\ell_+)\,\psi_{Z_+}^{(\theta_+(\ell_+))}(x_+,\ell_+)}{\bar{\psi}_{Z_+}^{(\xi,\theta_+)}(\ell_+)}, \tag{29}$$

$$\psi_{Z_+}(x,\ell) = \begin{cases}\frac{P_{\mathrm{D}}(x,\ell)g_+\left(z_+^{\theta(\ell)}|x,\ell\right)g_+\left(z_{\mathrm{e},+}^{\theta(\ell)}|x,\ell\right)}{\lambda c\left(z_+^{\theta(\ell)}\right)c\left(z_{\mathrm{e},+}^{\theta(\ell)}\right)}, & \theta(\ell)>0, \\ 1-P_{\mathrm{D}}(x,\ell), & \theta(\ell)=0.\end{cases} \tag{30}$$

Here, $\langle\cdot\rangle$ denotes the inner product, and $g_+\left(z_+^{\theta(\ell)}\mid\cdot\right)$ and $c\left(z_+^{\theta(\ell)}\right)$ represent the measurement likelihood and the clutter density of the kinetic state, respectively. $g_+\left(z_{\mathrm{e},+}^{\theta(\ell)}\mid\cdot\right)$ and $c\left(z_{\mathrm{e},+}^{\theta(\ell)}\right)$ denote the measurement and clutter likelihood functions of the EF, respectively. λ is the average clutter intensity.

The GLMB filter recursive process with EFs follows the efficient implementation in Vo et al. (2017). Ranked assignment and Gibbs sampling are used to efficiently generate GLMB components with high filtering weights, while maintaining diversity across the generated samples. For the state estimation of the multiple targets, we use a suboptimal marginal multi-objective estimator (Vo et al., 2014). The maximum a posteriori (MAP) cardinality estimate is first found from the cardinality distribution. Then, we extract the labels and average estimates of the multi-target states from the highest weighted component that has the same cardinality as the MAP cardinality estimate.

4 Simulations

In this section, we compare the tracking performances of the proposed EFs aided by GLMB and GLMB filters (Vo et al., 2017) under linear Gaussian conditions.

The size of the target surveillance region is $V = [-1000, 1000]\ \mathrm{m} \times [-1000, 0]\ \mathrm{m}$. Each target can be described by its state vector $\boldsymbol{x} = (x, \dot{x}, y, \dot{y})^{\mathrm{T}}$, which includes the positions and speeds of the x-axis and y-axis. Assume that the velocity of the target is nearly

constant, and its state equation can be given by

$$\boldsymbol{x}_k = \begin{bmatrix} 1 & T_\mathrm{s} & 0 & 0 \\ 0 & 1 & 0 & 0 \\ 0 & 0 & 1 & T_\mathrm{s} \\ 0 & 0 & 0 & 1 \end{bmatrix} \boldsymbol{x}_{k-1} + \begin{bmatrix} \frac{T_\mathrm{s}^2}{2} & 0 \\ T_\mathrm{s} & 0 \\ 0 & \frac{T_\mathrm{s}^2}{2} \\ 0 & T_\mathrm{s} \end{bmatrix} \boldsymbol{\mu}_{k-1}, \tag{31}$$

where $T_\mathrm{s} = 1$ s is the sampling period. $\boldsymbol{\mu}_{k-1}$ is state process noise and its covariance matrix is

$$\boldsymbol{Q}_{k-1} = \begin{bmatrix} \sigma^2 & 0 \\ 0 & \sigma^2 \end{bmatrix}, \tag{32}$$

where $\sigma = 2\ \mathrm{m/s^2}$. In the simulations, the EFs are $\boldsymbol{e}_k = (\mathrm{rf}_k, \mathrm{prf}_k, \mathrm{pw}_k)^\mathrm{T}$. Their specific parameter settings, which are unknown in our algorithm, are shown in Table 1. Take RF as an example to illustrate the meaning of stagger, agility, and jitter in Table 1.

Stagger uses two or more RF features to form a set $\{\mathrm{rf}_1, \mathrm{rf}_2, \cdots, \mathrm{rf}_{m_\mathrm{e}}\}$, where m_e is the number of elements. The RF features are repeatedly generated by

$$\mathrm{rf}_k = \mathrm{rf}_i, \quad i = k \bmod m_\mathrm{e}. \tag{33}$$

RF jitter is given by $\mathrm{rf}_k = \mathrm{rf}_0 + \varepsilon$, where rf_0 is the mean of the feature and $\varepsilon = [-\varsigma, \varsigma]$ follows a Gaussian distributed random variable. ς is the maximum jitter for the feature, set to 5%.

Agility means that the carrier frequency of adjacent pulses changes rapidly and randomly within a certain frequency band, and its model is

$$\mathrm{rf}_k = \mathrm{rf}_0 + \frac{B_\mathrm{s}}{2} \sin\left(2\pi k f T_\mathrm{r} + \varphi_0\right), \tag{34}$$

where B_s is the slip bandwidth, f is the agile frequency, T_r is the arrival time, and φ_0 is the initial phase.

The measurement equations of the target are

$$\boldsymbol{z}_k = \begin{bmatrix} 1 & 0 & 0 & 0 \\ 0 & 0 & 1 & 0 \end{bmatrix} \boldsymbol{x}_k + \boldsymbol{w}_k, \tag{35}$$

$$\boldsymbol{e}'_k = \boldsymbol{e}_k + \boldsymbol{w}^\mathrm{e}_k, \tag{36}$$

where $\boldsymbol{e}'_k$ is the EF measurement, $\boldsymbol{e}_k$ is the EF, and $\boldsymbol{w}_k$ and $\boldsymbol{w}^\mathrm{e}_k$ are the zero mean Gaussian noises with covariance matrices

$$\boldsymbol{R}_k = \begin{bmatrix} \sigma_x^2 & 0 \\ 0 & \sigma_y^2 \end{bmatrix}, \quad \boldsymbol{R}^\mathrm{e}_k = \begin{bmatrix} \sigma_\mathrm{rf}^2 & 0 & 0 \\ 0 & \sigma_\mathrm{prf}^2 & 0 \\ 0 & 0 & \sigma_\mathrm{pw}^2 \end{bmatrix}. \tag{37}$$

Here $\sigma_x = \sigma_y = 10$ m, $\sigma_\mathrm{rf} = 30$ MHz, $\sigma_\mathrm{prf} = 5$ kHz, and $\sigma_\mathrm{pw} = 10$ μs.

The resolution of the feature is the variance of the measurement noise. The probability of target detection is $p_{\mathrm{D},k} = 0.98$. The simulation time is $T = 100$ s. Clutter can be generated according to a Poisson point-process with $\mathcal{K}_k(z) = \lambda V c(z)$, where λ is the average number of clutters per scan, V is the surveillance region, and $c(z)$ is the spatial distribution of clutter, which is assumed to be uniform in the surveillance region. RF, PRF, and PW of the clutter are uniformly distributed in [0, 5000] MHz, [0, 1000] kHz, and [0, 1000] μs, respectively. The target survival probability is $p_{\mathrm{s},k} = 0.99$, and the birth model is an LMB RFS with $\pi_\mathrm{b} = \left\{r_\mathrm{b}^{(i)}, p_\mathrm{b}^{(i)}\right\}_{i=1}^{4}$, where $r_\mathrm{b} = 0.03$ and $p_\mathrm{b}^{(i)} = \delta\left(\boldsymbol{e}_\mathrm{b} - \boldsymbol{e}_\mathrm{b}^{(i)}\right) \mathcal{N}\left(\boldsymbol{x}; \boldsymbol{m}_\mathrm{b}^{(i)}, \boldsymbol{P}_\mathrm{b}\right)$ with $\boldsymbol{m}_\mathrm{b}^{(1)} = [0,0,0,0]^\mathrm{T}$, $\boldsymbol{m}_\mathrm{b}^{(2)} = [400,0,-600,0]^\mathrm{T}$, $\boldsymbol{m}_\mathrm{b}^{(3)} = [-800,0,-200,0]^\mathrm{T}$, $\boldsymbol{m}_\mathrm{b}^{(4)} = [-200,0,800,0]^\mathrm{T}$, $\boldsymbol{P}_\mathrm{b} = \mathrm{diag}\,(10,10,10,10)^2$. $\boldsymbol{e}_\mathrm{b}^{(i)}$ is the cluster center of EFs and is randomly initialized according to the solution result in Section. 3.1.1. In the proposed method, the weighted form of FCM is $m = 5$.

As for the tracking performance evaluation, we use the optimal subpattern assignment (OSPA) metric (Schuhmacher et al., 2008), whose cut-off is c_OSPA =100 and norm order is p_OSPA=100. For each case, we perform 100 Monte–Carlo (MC) simulations.

Table 1 Signal features of the emitters

Emitter	Working state	Radio frequency (MHz)	Pulse repetition frequency (kHz)	Pulse width (μs)
1	1	1000–1200 (Agility)	10–15 (Stagger)	320–360 (Stagger)
	2	1200 (Jitter)	20 (Jitter)	265–315 (Agility)
	3	1300–1400 (Stagger)	25 (Jitter)	320–360 (Agility)
2	1	1400 (Jitter)	30 (Jitter)	415–465 (Agility)
3	1	1500–1600 (Stagger)	35 (Jitter)	280–320 (Agility)
	2	1700 (Jitter)	35–40 (Agility)	320–370 (Stagger)
	3	1800–1900 (Agility)	35 (Jitter)	370–420 (Agility)
4	1	2000 (Jitter)	40–45 (Stagger)	225–275 (Agility)

Agility, jitter, and stagger in the bracket are the modulation types of the emitter features

The cluster center features after dynamic clustering based on the data field are shown in Fig. 2. It can be seen that there are seven cluster centers after clustering, and the EFs of each cluster center are shown in Table 2.

The trajectory of the target is shown in Fig. 3. These trajectories with cluttered measurements and position estimates from a single simulation are shown in Fig. 4 (150 clutter returns per scan over the region). The born time of targets 1, 2, and 3 is the same, $k = 1$ s. Target 4 is born at $k = 20$ s. Targets 1 and 3 die at time $k = 70$ s, and targets 2 and 4 die at time $k = 100$ s. It can be seen from Fig. 4 that the proposed method has satisfactory tracking performance in the cluttered environment.

To verify the advantages of the proposed method, it is compared with the GLMB filter (Vo et al., 2017) with the same clutter density (150 clutter returns per scan over the region). Figs. 5 and 6 show the cardinality estimation and OSPA distance of the proposed method and GLMB filter over the time, respectively. It can be seen that the proposed method has significant advantages.

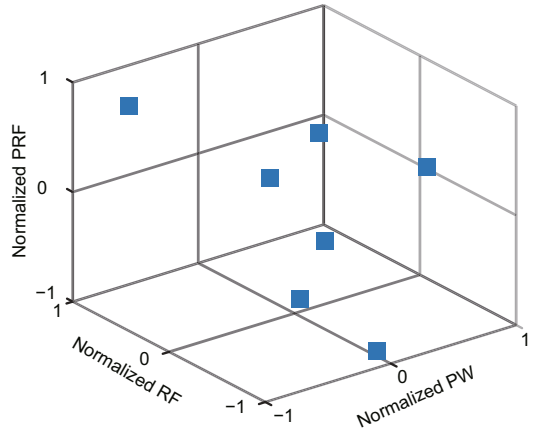

Fig. 2 Dynamic clustering based on the data field

PW: pulse width; RF: radio frequency; PRF: pulse repetition frequency

Table 2 Features of each cluster center

Cluster center	PW (μs)	RF (MHz)	PRF (kHz)
1	252.62	2257.74	42.61
2	293.13	1251.42	21.06
3	300.10	1553.09	36.39
4	339.00	1446.63	25.92
5	339.20	1055.36	12.64
6	375.65	1803.17	36.91
7	441.85	1509.07	31.48

PW: pulse width; RF: radio frequency; PRF: pulse repetition frequency

To further verify the anti-clutter performance of the proposed method, the average OSPA distances of the proposed method and GLMB filter are compared under different clutter intensities. As shown in Fig. 7, the average OSPA distance of the GLMB filter increases rapidly with increasing clutter intensity, while the average OSPA distance of the proposed method increases slowly. This indicates that the performance of the GLMB filter is susceptible

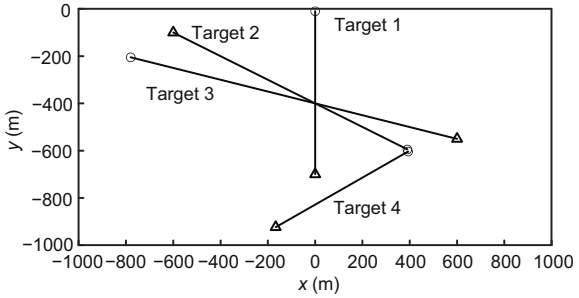

Fig. 3 Target trajectories

At "◯" locations, targets are born and at "△" locations, targets die

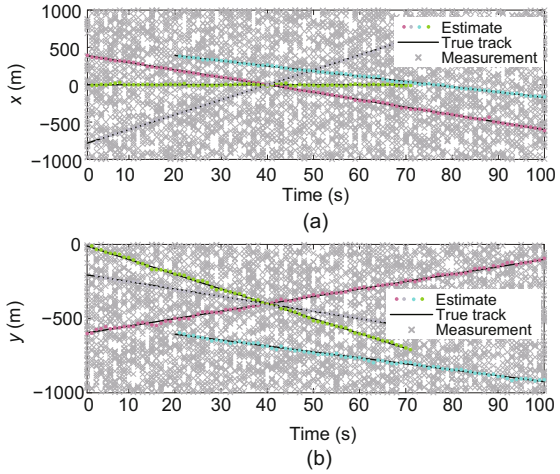

Fig. 4 True target positions and position estimates on x (a) and y (b) coordinates

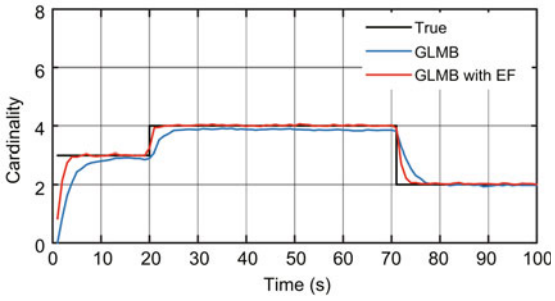

Fig. 5 Cardinality estimation of the GLMB and the GLMB with the EF filter

GLMB: generalized labeled multi-Bernoulli; EF: emitter feature

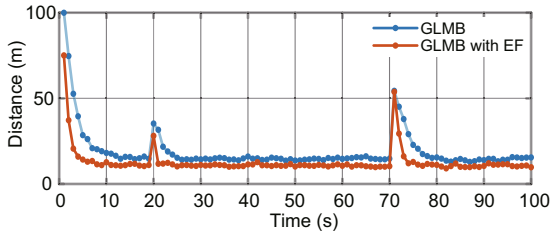

Fig. 6 OSPA distance of the GLMB and GLMB with the EF filter

OSPA: optimal subpattern assignments; GLMB: generalized labeled multi-Bernoulli; EF: emitter feature

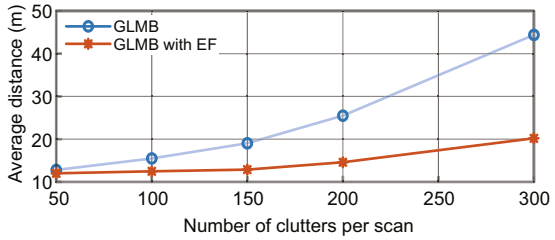

Fig. 7 Average OSPA distance vs. the number of clutters per scan

EF: emitter feature; GLMB: generalized labeled multi-Bernoulli; OSPA: optimal subpattern assignments

to the clutter, while the proposed method is less susceptible to the clutter (i.e., it has stronger resistance to the clutter).

In summary, the proposed method has not only satisfactory multi-target tracking performance, but also satisfactory anti-clutter performance.

5 Conclusions

This paper proposes an improved GLMB filter that integrates unknown and time-varying features of the emitter signals. It employs the feature information of the emitter to enhance the discrimination between the target and the clutter. It can be seen from the simulation results that the proposed method has significant performance advantages compared with the GLMB filter in heavy clutter scenarios.

Contributors

Qiang GUO and Long TENG designed the research and addressed the problems. Long TENG processed the data and drafted the paper. Xinliang WU and Dayu HUANG helped with the technical information. Wenming SONG supervised the study and helped organize the paper. Qiang GUO and Long TENG revised and finalized the paper.

Compliance with ethics guidelines

Qiang GUO, Long TENG, Xinliang WU, Wenming SONG, and Dayu HUANG declare that they have no conflict of interest.

References

Bar-Shalom Y, Kirubarajan T, Gokberk C, 2005. Tracking with classification-aided multiframe data association. *IEEE Trans Aerosp Electron Syst*, 41(3):868-878. https://doi.org/10.1109/TAES.2005.1541436

Battistelli G, Chisci L, Fantacci C, et al., 2013. Consensus CPHD filter for distributed multitarget tracking. *IEEE J Sel Top Signal Process*, 7(3):508-520. https://doi.org/10.1109/JSTSP.2013.2250911

Cao CH, Zhao YB, 2022. Range estimation based on symmetry polynomial aided Chinese remainder theorem for multiple targets in a pulse Doppler radar. *Front Inform Technol Electron Eng*, 23(2):304-316. https://doi.org/10.1631/FITEE.2000418

Chen HM, Li XR, Bar-Shalom Y, 2004. On joint track initiation and parameter estimation under measurement origin uncertainty. *IEEE Trans Aerosp Electron Syst*, 40(2):675-694. https://doi.org/10.1109/TAES.2004.1310013

Chen HM, Kirubarajan T, Bar-Shalom Y, 2008. Tracking of spawning targets with multiple finite resolution sensors. *IEEE Trans Aerosp Electron Syst*, 44(1):2-14. https://doi.org/10.1109/TAES.2008.4516985

Clark D, Ristic B, Vo BN, et al., 2010. Bayesian multi-object filtering with amplitude feature likelihood for unknown object SNR. *IEEE Trans Signal Process*, 58(1):26-37. https://doi.org/10.1109/TSP.2009.2030640

Da K, Li TC, Zhu YF, et al., 2020. Gaussian mixture particle jump-Markov-CPHD fusion for multitarget tracking using sensors with limited views. *IEEE Trans Signal Inform Process Netw*, 6:605-616. https://doi.org/10.1109/TSIPN.2020.3016478

Da K, Li TC, Zhu YF, et al., 2021. Recent advances in multisensor multitarget tracking using random finite set. *Front Inform Technol Electron Eng*, 22(1):5-24. https://doi.org/10.1631/FITEE.2000266

Guo Q, Nan PL, Wan J, 2016. Signal classification method based on data mining for multi-mode radar. *J Syst Eng Electron*, 27(5):1010-1017. https://doi.org/10.21629/JSEE.2016.05.09

Guo YF, Fan KS, Peng DL, et al., 2015. A modified variable rate particle filter for maneuvering target tracking. *Front Inform Technol Electron Eng*, 16(11):985-994. https://doi.org/10.1631/FITEE.1500149

Guo YF, Tharmarasa R, Rajan S, et al., 2016. Passive tracking in heavy clutter with sensor location uncertainty. *IEEE Trans Aerosp Electron Syst*, 52(4):1536-1554. https://doi.org/10.1109/TAES.2016.140820

Guo YF, Li Y, Ren X, et al., 2020a. Multiple maneuvering extended target tracking based on Gaussian process. *Acta Autom Sin*, 46(11):2392-2403 (in Chinese). https://doi.org/10.16383/j.aas.c180849

Guo YF, Li Y, Xue AK, et al., 2020b. Simultaneous tracking of a maneuvering ship and its wake using Gaussian processes. *Signal Process*, 172:107547. https://doi.org/10.1016/j.sigpro.2020.107547

Herrmann M, Hermann C, Buchholz M, 2021. Distributed implementation of the centralized generalized labeled

multi-Bernoulli filter. *IEEE Trans Signal Process*, 69:5159-5174. https://doi.org/10.1109/TSP.2021.3107632

Jin B, Li C, Guo J, et al., 2019. Multi-target tracking in clutter aided by Doppler information. *J Univ Electron Sci Technol China*, 48(4):511-517 (in Chinese). https://doi.org/10.3969/j.issn.1001-0548.2019.04.006

Li TC, Hlawatsch F, 2021. A distributed particle-PHD filter using arithmetic-average fusion of Gaussian mixture parameters. *Inform Fus*, 73:111-124. https://doi.org/10.1016/j.inffus.2021.02.020

Li TC, Sun SD, Bolić M, et al., 2016. Algorithm design for parallel implementation of the SMC-PHD filter. *Signal Process*, 119:115-127. https://doi.org/10.1016/j.sigpro.2015.07.013

Li TC, Su JY, Liu W, et al., 2017. Approximate Gaussian conjugacy: parametric recursive filtering under nonlinearity, multimodality, uncertainty, and constraint, and beyond. *Front Inform Technol Electron Eng*, 18(12):1913-1939. https://doi.org/10.1631/FITEE.1700379

Li TC, Prieto J, Fan HQ, et al., 2018. A robust multi-sensor PHD filter based on multi-sensor measurement clustering. *IEEE Commun Lett*, 22(10):2064-2067. https://doi.org/10.1109/LCOMM.2018.2863387

Li TC, Liu Z, Pan Q, 2019. Distributed Bernoulli filtering for target detection and tracking based on arithmetic average fusion. *IEEE Signal Process Lett*, 26(12):1812-1816. https://doi.org/10.1109/LSP.2019.2950588

Liu C, Sun JP, Lei P, 2018. δ-generalized labeled multi-Bernoulli filter using amplitude information of neighboring cells. *Sensors*, 18(4):1153. https://doi.org/10.3390/s18041153

Mahler R, 2007. PHD filters of higher order in target number. *IEEE Trans Aerosp Electron Syst*, 43(4):1523-1543. https://doi.org/10.1109/TAES.2007.4441756

Mahler RPS, 2003. Multitarget Bayes filtering via first-order multitarget moments. *IEEE Trans Aerosp Electron Syst*, 39(4):1152-1178. https://doi.org/10.1109/TAES.2003.1261119

Mahler RPS, 2007. Statistical Multisource-Multitarget Information Fusion. Artech House, Norwood, USA.

Peng H, Huang G, Tian W, et al., 2018. Labeled multi-Bernoulli filter based on amplitude information. *Syst Eng Electron*, 40(12):2636-2641. https://doi.org/10.3969/j.issn.1001-506X.2018.12.03

Ristic B, Vo BT, Vo BN, et al., 2013. A tutorial on Bernoulli filters: theory, implementation and applications. *IEEE Trans Signal Process*, 61(13):3406-3430. https://doi.org/10.1109/TSP.2013.2257765

Schuhmacher D, Vo BT, Vo BN, 2008. A consistent metric for performance evaluation of multi-object filters. *IEEE Trans Signal Process*, 56(8):3447-3457. https://doi.org/10.1109/TSP.2008.920469

Sun X, Li RW, Zhou LS, 2020. Multidimensional information fusion in active sonar via the generalized labeled multi-Bernoulli filter. *IEEE Access*, 8:211335-211347. https://doi.org/10.1109/ACCESS.2020.3039347

Vo BN, Ma WK, 2006. The Gaussian mixture probability hypothesis density filter. *IEEE Trans Signal Process*, 54(11):4091-4104. https://doi.org/10.1109/TSP.2006.881190

Vo BN, Vo BT, Phung D, 2014. Labeled random finite sets and the Bayes multi-target tracking filter. *IEEE Trans Signal Process*, 62(24):6554-6567. https://doi.org/10.1109/TSP.2014.2364014

Vo BN, Vo BT, Hoang HG, 2017. An efficient implementation of the generalized labeled multi-Bernoulli filter. *IEEE Trans Signal Process*, 65(8):1975-1987. https://doi.org/10.1109/TSP.2016.2641392

Wang LP, Zhan RH, Huang Z, et al., 2021. Joint tracking and classification of extended targets with complex shapes. *Front Inform Technol Electron Eng*, 22(6):839-861. https://doi.org/10.1631/FITEE.2000061

Wu WH, Cai YC, Jin HB, et al., 2021. Derivation of the multi-model generalized labeled multi-Bernoulli filter: a solution to multi-target hybrid systems. *Front Inform Technol Electron Eng*, 22(1):79-87. https://doi.org/10.1631/FITEE.2000105

Yi W, Chai L, 2021. Heterogeneous multi-sensor fusion with random finite set multi-object densities. *IEEE Trans Signal Process*, 69:3399-3414. https://doi.org/10.1109/TSP.2021.3087033

Yi W, Jiang M, Hoseinnezhad R, 2017. The multiple model Vo-Vo filter. *IEEE Trans Aerosp Electron Syst*, 53(2):1045-1054. https://doi.org/10.1109/TAES.2017.2667300

Yi W, Li GC, Battistelli G, 2020. Distributed multi-sensor fusion of PHD filters with different sensor fields of view. *IEEE Trans Signal Process*, 68:5204-5218. https://doi.org/10.1109/TSP.2020.3021834

Zhou YQ, Zhu SL, 2015. GM-PHD filter with signal features of emitter. *Asian J Contr*, 17(5):1978-1983. https://doi.org/10.1002/asjc.1040

Zhu Y, Liang S, Wu XJ, et al., 2021. A random finite set based joint probabilistic data association filter with non-homogeneous Markov chain. *Front Inform Technol Electron Eng*, 22(8):1114-1126. https://doi.org/10.1631/FITEE.2000209

Zhu YQ, 2015. Research on Tracking Techniques of Multiple Radar Emitter Targets Based on PHD Filter. PhD Thesis, National University of Defense Technology, Changsha, China (in Chinese).